Solar Energy Materials and Solar Cells 194 (2019) 142–147

Contents lists available at ScienceDirect

Solar Energy Materials and Solar Cells

journal homepage: www.elsevier.com/locate/solmat

Spectral characterization of solar cells and modules using LED-based solar simulators

M. Turek[a,*], K. Sporleder[a,b], T. Luka[a,c]

[a] Fraunhofer Center for Silicon Photovoltaics CSP, Otto Eissfeldt Str. 12, D-06120 Halle (Saale), Germany
[b] Leipzig University of Applied Sciences (HTWK), Karl-Liebknecht-Str. 132, D-04277 Leipzig, Germany
[c] Anhalt University of Applied Sciences, Bernburger Str. 55, D-06366 Köthen, Germany

ARTICLE INFO

Keywords:
Quantum efficiency
Reflectivity
Solar simulator
LED

ABSTRACT

The failure and loss analysis of solar cells relies on the precise determination of their electrical performance parameters. Light emitting diodes (LEDs) used as light sources in solar simulators provide a number of advantages compared to conventional Xenon-based solar simulators. In this work, we present an approach to rapidly measure the quantum efficiency and the reflectivity that takes the spectral broadening of the LEDs fully into account. Our approach does not rely on any specific shape of the spectral peaks and can thus be applied to any type of quasi-monochromatic light source. The two proposed methods yield valuable additional information on the solar cell performance and material properties that cannot be obtained by conventional solar simulators. Using LED solar simulators, they are completely in-line capable as they can be performed in less than one second.

1. Introduction

Solar simulators are major characterization tools yielding the performance values of solar cells or modules when no spatial information on local solar cell properties is required. In recent years, the properties and capabilities of solar simulators using light emitting diodes (LEDs) as a light source have intensely been studied [1–4] while the first commercially available systems are increasingly entering the market. These light sources can be designed such that they provide a very high conformity with norm spectra, i.e. the AM1.5 spectrum. Additionally, LED-based solar simulators also provide a number of properties that allow measurement approaches going beyond the standardized current-voltage-characterization. They come with a very high variability concerning the illumination intensity, the spectral composition of the light, and the duration of the flash and the measurements. Each of these properties can be utilized to develop advanced measurement approaches yielding valuable additional information on the performance and possible loss mechanisms within a solar cell or module [5,6,7,8].

A major advantage of LED-based solar simulators compared to conventional systems is their flexibility in the illumination spectrum. Thus, this type of measurement system can be used to obtain spectral information such as the solar cell's external quantum efficiency or it's reflectivity $R(\lambda)$ in dependence of the wavelength λ. It has been shown, that quantum efficiency measurements can be obtained using LED light sources with a lock-in method when a number of error corrections are implemented, i.e. corrections for the spectral band width or spatial irradiance distribution. [9] In our work, we present a rapid EQE measurement and data analysis scheme as well as an approach to determine the spectral reflectivity. In contrast to conventional measurement approaches to determine the spectral properties of a solar cell, the LED-spectra are rather broad with a spectral width between 20 nm and 100 nm. Hence, it is very important to account for these broad emission spectra. Correcting finite bandwidths in spectral measurements has been addressed in the context of slit functions previously by a number of publications. A correction scheme for a special set of triangular slit functions has been presented in [10] and extended to a wider class of slit functions in [11]. We propose a mathematical framework that accounts for this spectral broadening independently of the exact shape of the individual LED-spectra. Our approach extends earlier methods in two ways: First, we show that self-consistent iterations improve the result significantly and second, we include a correction independent on the specific shape of the spectra on both values in the data points $[\lambda, \mathrm{EQE}(\lambda)]$. Furthermore, we show that this approach is applicable to commercially available LED solar simulators. It allows for a very rapid measurement using with significantly reduced measurement uncertainties making an in-line application in a solar cell production possible.

Based on the spectral measurements of and $R(\lambda)$, a detailed loss analysis can be performed. For example, front and rear side losses can be distinguished from bulk losses [12]. Furthermore, the reflectivity as

* Corresponding author.
E-mail address: marko.turek@csp.fraunhofer.de (M. Turek).

https://doi.org/10.1016/j.solmat.2019.02.007
Received 9 October 2018; Received in revised form 16 January 2019; Accepted 9 February 2019
Available online 18 February 2019
0927-0248/

a function of the wavelength can be employed to quantify the thickness of the anti-reflective coating on the front side. Thus, various causes in a cell production process that can lead to performance losses can be identified based on the quantum efficiency and reflectivity testing. As our method is formulated in a rather general mathematical way, its application can be directly extended to filter-based systems or other light sources where a finite bandwidth is present.

For these spectral applications, we will first develop a mathematical framework. Its major assumptions are discussed in Section 2 and a mathematically sound formulation for the analysis of experimental measurement data is given. We will demonstrate the applicability of our data analysis approach to realistic numerical test data in Section 3. Furthermore, we discuss the influence of the individual spectral peak shapes on the resulting experimental data. Finally, we apply our methods to different solar cells in Section 4. In particular, we will discuss the resulting EQE and reflectivity-values in the context of crystalline silicon solar cells, and CIGS thin film modules.

2. Mathematical model and theoretical considerations

The generated current of a solar cell, I_{gen}, is related to the solar cell's external quantum efficiency and the spectral flux density $S(\lambda)$, i.e.

$$I_{\text{gen}} = \frac{q}{hc} \int \mathrm{d}\lambda \; S(\lambda)\, \lambda \; \mathrm{EQE}(\lambda) \tag{1}$$

with λ being the wavelength.

A rapid EQE-test based on LED-solar simulators relies on the subsequent illumination with the individual LED channels and the measurement of the corresponding short circuit current of the solar cell. Each channel is characterized by an channel-specific spectral flux density $S_{n=1\ldots N}(\lambda)$ of finite spectral width. For each channel n, this flux density leads to a solar cell short circuit current $I_{\text{gen,n}}$ according to Eq. (1), which can be written as

$$I_{\text{gen,n}} = <\lambda \; \mathrm{EQE}(\lambda)>_n \tag{2}$$

in terms of the generalized averages $\langle \ldots \rangle_n$ defined for any function $f(\lambda)$ as

$$<f(\lambda)>_n \equiv \frac{q}{hc} \int \mathrm{d}\lambda \; S_n(\lambda) f(\lambda)\,. \tag{3}$$

The calculation of these averages for each spectral peak of the LEDs does not require any assumption on the peak shape nor any fitting, e.g. using Gaussians. In terms of these averages, the mean value $\bar{\lambda}_n$ determined by a spectral peak $S_n(\lambda)$ is given by the first moment $\langle \lambda^1 \rangle_n$, i.e. $f(\lambda) = \lambda$, and the standard deviation σ_n by the second moment $\langle \lambda^2 \rangle_n$ of the broad-band flux density $S_n(\lambda)$. In particular, one finds for any peak shape $S_n(\lambda)$

$$\bar{\lambda}_n = \frac{<\lambda>_n}{<1>_n} \quad \text{and} \quad \sigma_n^2 = \frac{\langle \lambda^2 \rangle_n}{\langle 1 \rangle_n} - \bar{\lambda}_n^{\,2}\,. \tag{4}$$

The zeroth moment $\langle \lambda^0 \rangle_n = \langle 1 \rangle_n$ is just a constant prefactor determined by the total spectral flux. In an experiment, it can be obtained using a calibrated reference cell. The standard deviations σ_n are quantitative measures for the spectral widths of the spectral flux densities $S_{n=1\ldots N}(\lambda)$. For a very narrow peak, the standard deviation vanishes, i.e. $\sigma_n \to 0$.

Based on these moments of the spectral peaks, one can develop a systematic mathematical framework using a series expansion in terms of the small parameter $\sigma_n/\bar{\lambda}_n \ll 1$ which is independent of the shape of the peaks $S_{n=1\ldots N}(\lambda)$. The goal of an EQE-measurement is to obtain N pairs $[\lambda_n;\, \mathrm{EQE}_n]$ that represent the underlying quantum efficiency and which can be calculated from the measured data for each of the $n = 1\ldots N$ LED channels. If the spectral flux density would be very sharply peaked around a wavelength λ_n, i.e. $S_n(\lambda) \sim \delta(\lambda - \lambda_n)$ such that $\sigma_n \to 0$, then Eq. (2) would immediately give

$$I_{\text{gen,n}} = <1>_n \;\; \lambda_n \; \mathrm{EQE}(\lambda_n) \tag{5}$$

with λ_n just being the center wavelength where $S_n(\lambda)$ reaches its maximum. In this case, the pair of values $[\lambda_n;\, \mathrm{EQE}_n \approx -I_{\text{sc,n}} / (\lambda_n \langle 1 \rangle_n)]$ would exactly represent the external quantum efficiency based on the experimentally accessible values $I_{\text{sc,n}}$ and $\langle 1 \rangle_n$. This corresponds to the standard approach for conventional EQE measurements with monochromatic illumination.

However, for a spectrally broad peak $I_n(\lambda)$ with $\sigma_n > 0$, one has to account for the integration in Eq. (2) which includes a broad wavelength range. Furthermore, one has to identify the correct corresponding wavelength λ_n in the pairs $[\lambda_n;\, \mathrm{EQE}_n]$. Naturally, an error in λ_n leads to large deviations in those regions where the quantum efficiency has a large slope. Thus, the slope of the quantum efficiency has to enter the data analysis when the measurement is performed using peaks with finite spectral width. For an LED-based light source, one can nevertheless assume that the peaks $S_n(\lambda)$ are rather narrow in the sense that $\bar{\lambda}_n \gg \sigma_n > 0$, even if the peak's width is finite.

Ideally, solution Eq. (5) can also be applied to the case of finite spectral width with $\bar{\lambda}_n \gg \sigma_n > 0$. Thus, one has to find the two values λ'_n and λ''_n that fullfill the relation

$$\begin{aligned} I_{\text{gen,n}} &= <\lambda \; \mathrm{EQE}(\lambda)>_n \\ &\approx <1>_n \;\; \lambda'_n \; \mathrm{EQE}(\lambda''_n)\,, \end{aligned} \tag{6}$$

in analogy to Eq. (5). Comparing Eq. (2) with Eq. (6), one finds the solution

$$\begin{aligned} \lambda'_n &= \frac{<\lambda>_n}{<1>_n} = \bar{\lambda}_n \quad \text{and} \\ \lambda''_n &= \frac{<\lambda^2>_n}{<\lambda>_n} = \bar{\lambda}_n \left\{ 1 + \left(\frac{\sigma_n}{\bar{\lambda}_n} \right)^2 \right\} \end{aligned} \tag{7}$$

by a series expansion of if higher than first order derivatives of the quantum efficiency are neglected. This results means, that the value $\mathrm{EQE}_n = \mathrm{EQE}(\lambda''_n)$ is not evaluated at $\bar{\lambda}_n$ but at a larger value. The shift in wavelength relative to $\bar{\lambda}_n$ is determined by the width of the peak, i.e. the ratio $\sigma_n/\bar{\lambda}_n$. It will be shown, that this correction is of particular importance for non-symmetric peaks $S_n(\lambda)$. The pairs of λ_n and EQE_n values are thus given by analyzing the spectral flux densities $S_n(\lambda)$ and the corresponding short circuit currents $I_{\text{gen,n}}$:

$$\left[\lambda_n;\, \mathrm{EQE}_n \right] \to \left[\bar{\lambda}_n \left\{ 1 + \left(\frac{\sigma_n}{\bar{\lambda}_n} \right)^2 \right\};\, \frac{I_{\text{gen,n}}}{\bar{\lambda}_n \; <1>_n} \right] \tag{8}$$

This solution is exact if the quantum efficiency would have vanishing higher derivatives, i.e. $\mathrm{d}^k\mathrm{EQE}/\mathrm{d}\lambda^k \to 0$ for $k > 1$. This is typically the case for the plateau in an intermediate wavelength range. For smaller and larger wavelengths, there is a steep rise of the quantum efficiency implying a finite non-zero curvature of the EQE-curve, i.e. $\mathrm{d}^2\mathrm{EQE}(\lambda)/\mathrm{d}\lambda^2 \neq 0$. In this case, one finds a correction to the EQE-value in solution (8) in the form of

$$\mathrm{EQE}(\lambda''_n) = \frac{I_{\text{gen,n}}}{\bar{\lambda}_n \; <1>_n} \left\{ 1 + \frac{1}{2 I_{\text{gen,n}}} \frac{\mathrm{d}^2\mathrm{EQE}(\lambda)}{\mathrm{d}\lambda^2} \left[\frac{<\lambda^2>_n^2}{<\lambda>_n} - <\lambda^3>_n \right] \right\} \tag{9}$$

$$\approx \frac{I_{\text{gen,n}}}{\bar{\lambda}_n \; <1>_n} \left\{ 1 - \frac{<1>_n}{2 I_{\text{gen,n}}} \frac{\mathrm{d}^2\mathrm{EQE}(\lambda)}{\mathrm{d}\lambda^2} \bar{\lambda}_n \, \sigma_n^2 \right\} \tag{10}$$

$$\approx \frac{I_{\text{gen,n}}}{\bar{\lambda}_n \; <1>_n} \left\{ 1 - \frac{1}{2} \frac{1}{\mathrm{EQE}(\lambda''_n)} \frac{\mathrm{d}^2\mathrm{EQE}(\lambda)}{\mathrm{d}\lambda^2} \sigma_n^2 \right\} \tag{11}$$

leading to the pairs $[\lambda''_n,\, EQE(\lambda''_n)]$. This expression for $\mathrm{EQE}_n \equiv \mathrm{EQE}(\lambda''_n)$ together with Eq. (7) for λ''_n is the first central result of this work. It implies, that a precise calculation of the unknown quantum efficiency requires the knowledge of the moments of the spectral peaks, i.e. $<\lambda^0> \ldots <\lambda^3>$, together with the second derivative, i.e. the curvature, of the quantum efficiency itself. It is valid for any peak shape as long as the peaks are not too broad while no assumption

concerning the shape of the peak has to be made. In particular, our approach is not restricted to Gaussian peaks. The curvature of $EQE(\lambda)$ that enters Eqs. (9)–(11) can be obtained by an iterative approach in which a) Eq. (8) is applied to obtain a first estimate of $EQE^{(0)}(\lambda)$, b) the second derivative $d^2EQE^{(0)}/d\lambda^2$ is calculated, and c) a new quantum efficiency value $EQE^{(1)}(\lambda)$ is determined using Eq. (9) or Eq. (10). This approach can be repeated a few times to obtain the final solution for the quantum efficiency.

The approximation in Eq. (10) neglects higher order contributions of $\sigma_n/\bar{\lambda}_n$. Hence, for rather narrow peaks with $\sigma_n/\bar{\lambda}_n \ll 1$, Eq. (10) can be used. Eventhough the error in the uncorrected EQE, Eq. (8), is small, it cannot be neglected. The iterative approach involving Eq. (9) works as long as the experimental setup is characterized by spectra with $d^2\mathrm{EQE}(\lambda)/d\lambda^2\ \sigma_n \ll 1$, as can be seen from Eq. (11). This is the case, as long as the spectral width over which the quantum efficiency rises or falls is smaller than the peak width of the channel which probes the cell at the same wavelength values.

The measurement of a cell's reflectivity using the LED-based light source together with a sensor, e.g. a camera, is very similar to the rapid quantum efficiency test described in the previous section. The same mathematical algorithms can be applied when the detector signal, i.e. its short circuit current, is written in terms of the reflectivity $R_{\mathrm{cell}}(\lambda)$ of the sample:

$$I_{\mathrm{detec,n}} = <\lambda\ R_{\mathrm{cell}}(\lambda)\ \mathrm{EQE}_{detec}(\lambda)>_n . \tag{12}$$

The pairs of values $[\lambda_n;\ \mathrm{R}_n]$ are then obtained from the experimental data by calculating

$$\left[\lambda_n;\ \mathrm{R}_n\right] \rightarrow \left[\bar{\lambda}_n\left\{1+\frac{\sigma_n^2}{\bar{\lambda}_n^2}\right\};\ \frac{I_{\mathrm{detec,n}}}{\bar{\lambda}_n\ \mathrm{EQE}_{\mathrm{detec,n}} < 1>_n}\right] \tag{13}$$

in analogy to Eqs. (8) and (9). The unknown quantum efficiency of the detector together with the spectral flux constant ($\mathrm{EQE}_{detec,n} < 1 >_n$) has to be measured using a calibrated reference cell with known reflectivity $R(\lambda)$. Once these calibration values are determined together with the spectral flux density $S_n(\lambda)$ of each channel, the reflectivity can be calculated using Eqs. (13) and (2). Subsequently, an iterative approach can be applied similarly to the EQE calculation.

3. Application to numerical data

In order to investigate the mathematical approach described in Section 2, we have generated model data for the quantum efficiency based on a commercially available solar cell. Furthermore, we have defined different types of LED spectra with varying width and skewness. These model spectra are calculated using a skew normal distribution. This distribution yields the Gaussian peak shape only in case of a symmetric peak. However, it is worthwhile to note that our approach is not limited to this group of functions as it requires only the moments of the peaks but not their precise shape.

In Fig. 1, we have investigated our approach for a symmetrically shaped peak with a width of about 60 nm. The peak shape is shown in the Fig. 1 together with the model-EQE-data. Assuming that the center of this peak shape is positioned at various wavelengths, the first estimation of the EQE according to Eq. (5) is represented by the red crosses. It can be observed that this first approximation which neglects the peak width yields rather reasonable results for wavelengths where the EQE is not changing to much. However, it can also be observed that there is a systematic error where the EQE shows a non-zero curvature. A small curvature, i.e. around 1000 nm and 1150 nm, yields only minor errors. On the other hand, a more pronounced curvature, i.e. around 350 nm and 450 nm, gives rather large deviations compared to the original EQE data. The maximal deviation $\Delta\mathrm{EQE}_{\mathrm{max}}$ from the original data is about 0.12 at $\lambda = 360$ nm. Applying our correction scheme, Eqs. (7) and (9), significantly reduces the error at these wavelengths. While the first iteration gives a rather good result already leading to a reduced

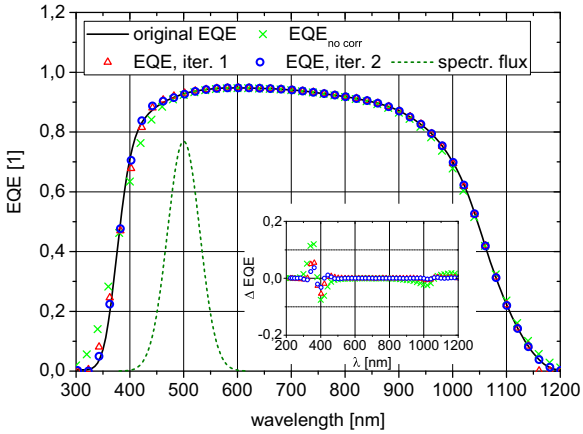

Fig. 1. The original cell EQE is shown by the black solid line while the symmetric peak shape under investigation with a width of 60 nm is shown as green dashed line. The position of the maximum of the peak is shifted over the wavelength range from 300 nm to 1200 nm. Application of Eq. (5) yields the red crosses as a first approximation of the EQE based on the broad spectral peak. Subsequent application of our correction scheme, Eqs. (7) and (9), for λ_n and EQE_n leads to the first iteration (red triangles) and second iteration (blue circles) of the EQE. The inset shows the deviation from the original cell EQE.

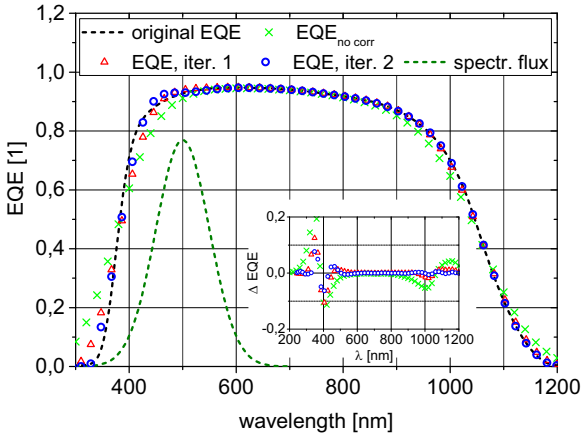

Fig. 2. Same data as in Fig. 1 for a symmetric peak with larger spectral width of 100 nm.

maximum deviation of $\Delta\mathrm{EQE}_{\mathrm{max}} = 0.054$, the second iteration appears to lead to very small measurement errors with $\Delta\mathrm{EQE}_{\mathrm{max}} = 0.037$.

This effect is even more pronounced for a broader peak shape as shown in Fig. 2. In this case, not only the short wavelength ascent around 400nm but also the long wavelength descent of the EQE around 1050nm is affected. Here, we find an error of $\Delta\mathrm{EQE}_{\mathrm{max}} = 0.22$. In both cases, our approach, Eqs. (7) and (9), can significantly improve the quality of the resulting EQE data. This implies that even a rather broad LED-peak can give reliable EQE-results leading to a significantly reduced deviation of $\Delta\mathrm{EQE}_{\mathrm{max}} = 0.12$ after the first iteration and $\Delta\mathrm{EQE}_{\mathrm{max}} = 0.076$ after the second iteration found at wavelength $\lambda = 340$ nm. As expected from the discussion in Section 2, the EQE values in the wavelength range of weakly changing EQE-values, i.e. between 500 nm and 900 nm, fit very well to the original data irrespective of the width of the peak.

In Fig. 3, we have investigated the impact of a unsymmetric peak shape on the resulting EQE data. The uncorrected EQE estimation based on Eq. (5) shows a systematic shift in the wavelengths of the resulting pairs $[\lambda_n,\ \mathrm{EQE}_n]$ that is due to the unsymmetry. This imposes a maximal error of $\Delta\mathrm{EQE}_{\mathrm{max}} = 0.28$ at $\lambda = 400$ nm. The correction scheme, Eqs. (7) and (9), gives a much better fit of the calculated EQE-data compared to the original EQE-data leading to a reduction of the maximal error

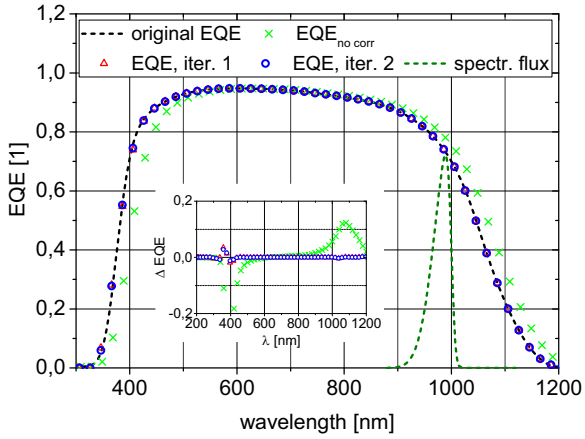

Fig. 3. Same data as in Fig. 1 for an unsymmetric peak.

$\Delta EQE_{max} = 0.035$ after the first iteration and $\Delta EQE_{max} = 0.027$ after the second iteration.

Summarizing, we found that the application of Eqs. (7) and (9) leads to a significant improvement of EQE-data obtained from broad spectral peaks. Our approach corrects an increasing peak width and an unsymmetric peak shape. It is independent of the exact form of the peak as only the first moments of the peaks enter the correction. In particular, it does not require fitting the LED peak shapes to any specific set of functions such as Gaussians.

4. Application to experimental results

In this section, we apply the rapid EQE test and the rapid reflectivity measurement to several types of solar cells. The measurements are performed using an Sinus 220 LED solar simulator by Wavelabs Solar Metrology Systems GmbH. This solar simulator features 21 LED channels in the range between 350 nm and 1050 nm. The peaks widths are between 20 nm and 100 nm. In Fig. 4, the shape of four typical spectra of individual LED channels are shown together with a typical EQE curve of a silicon solar cell. Each channel can be operated individually as necessary for the rapid EQE and reflectivity test. Reference data for the quantum efficiency and reflectivity are obtained using the loss analysis tool LOANA by pv tools GmbH. The measurements of the spectral response were performed as absolute measurements without application of a bias light. Thus, it is worthwhile to note, that for samples with a strong non-linearity of the current on the intensity, an EQE measurement of the reference cell and the samples at comparable intensities leads to a higher accuracy in the resulting data of the rapid EQE test.

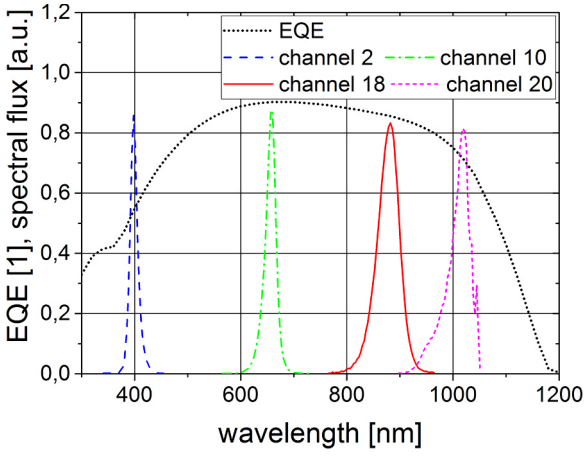

Fig. 4. Typical EQE curve of a multi-crystalline silicon solar cell in combination with four typical spectra of individual LED channels of the Sinus 220 LED solar simulator.

4.1. Rapid quantum efficiency test

In order to demonstrate our approach for the rapid full area quantum efficiency test, we have chosen silicon solar cells and CIGS mini-modules. A mono-crystalline silicon solar cell was used as a reference cell to determine the overall total spectral flux. i.e. $<\lambda^0>_n = <1>_n$, of each individual channel. It is worthwhile to note, that for the experimental setup, each LED channel is characterized by its individual spectral peak shape $S_n(\lambda)$. It is determined using an internal spectrometer that is integrated into the LED solar simulator. The rapid EQE data were determined according to Eq. (8). As the LED-based EQE measurement is a full area measurement which includes the optically inactive finger and busbar areas, a geometric scaling factor was determined taking the shading due to the different cell and mini-module layouts into account. This is necessary, as the LOANA measurements have been performed at and averaged over several spots of size 2 cm × 2 cm excluding the busbar areas. The scaling factor is thus obtained from the area coverage of the busbars of each cell.

Besides the in-line quality control of solar cells, the degradation analysis of cells or modules is a significant application case for EQE measurements. Hence, we have chosen neighbored multi-crystalline PERC solar cell showing pronounced light induced degradation. In Fig. 5, we present the EQE data of two silicon solar cells, one in the undegraded state and the other in the degraded state, with an power loss of 14%. For either case, we find a very close match between the reference EQE-data and the data obtained by our approach using the LED solar simulator. The difference between the two cell states is a pronounced loss of quantum efficiency in the long wavelengths larger than 700 nm. This EQE-loss due to the degradation is clearly reproduced by the LED solar simulator measurement.

As a second sample batch, CIGS mini-modules with different spectral responsivity were used. Our approach of the rapid EQE measurement generates a close match with a standard EQE measurement even with the different semiconductor material, as shown in Fig. 6. The EQE difference of the two samples in the long wavelengths larger than 900 nm is correctly reproduced as well.

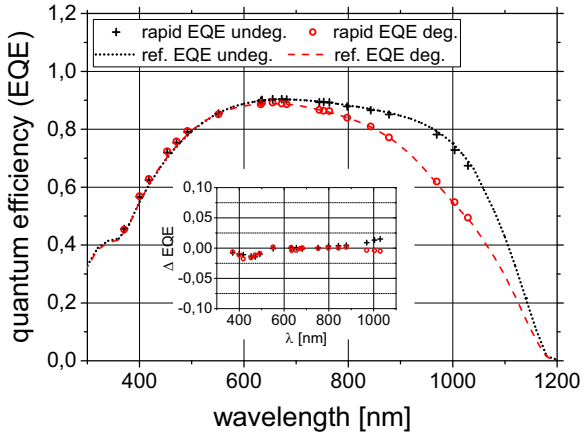

Fig. 5. Multi-crystalline PERC solar cells made from neighbored wafers, one in the initial state (black) and one in the LeTID degraded state (red). The EQE loss due to the degradation is well visible with our approach of rapid EQE measurement.

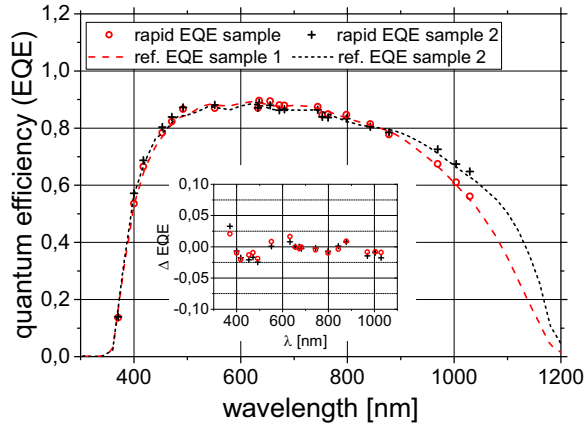

Fig. 6. CIGS mini-modules with different spectral responsivity. The EQE-data obtained with the LED solar simulator show a good match with the reference EQE-data.

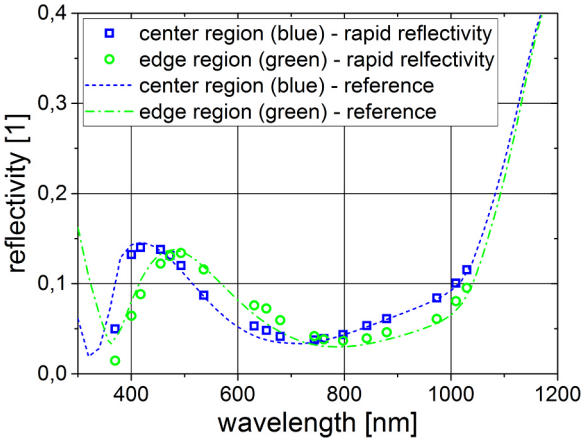

Fig. 8. Reflectivity of blue and green region of the test cell (indicated in Fig. 7).

4.2. Rapid reflectivity test

As described in Section 2, the reflectivity can be determined similarly to the rapid EQE test. In our experimental setup, we have employed the SINUS200 LED solar simulator together with an Andor Zyla sCMOS camera. The camera detects a spatial resolved intensity distribution of the reflected light of the test cell. In a first step, the spectral flux of each channel in combination with the spectral response of the camera have been determined using a reference cell, see Fig. 7 (left). The reflectivity data of the reference cell has been obtained using the LOANA cell loss analysis system. In the second step, a test cell with inhomogeneous anti-reflective SiN coating, see Fig. 7 (right), has been measured using our rapid full area reflectivity test. In either case, the background signal of the camera has been subtracted from the measured image. Due to the fixed camera position, only a certain part of the total reflected light has been measured. As this depends on the type of solar cell texturization, the usage of a comparable solar cell technology for the reference cell and the sample cells reduces the measurement errors. However, this does not impose any major limitations of our approach to an in-line application of the method as in production large numbers of solar cells of identical technology pass through the solar simulator test station. The overall measurement time yielding the data of 17 LED channels has been around 500 msec.

As can be observed in Fig. 8, the reflectivity data of the cell is rather well reproduced by the rapid reflectivity test. The two areas of different SiN coating thickness can well be distinguished in the resulting data. In particular, the shift in the position of the maxima and minima are well described by our test method. There is a smaller deviation at small wavelengths below 400 nm which can be attributed to the angle dependent reflectivity properties as the measurement in the reference tool (LOANA) is performed under a smaller angle than the rapid test using the LED solar simulator.

5. Discussion and conclusions

Spectral resolved measurements such as the determination of the quantum efficiency or reflectivity are valuable characterization approaches for the loss analysis of solar cells. Up to now, an inline implementation of the methods was not possible as the corresponding measurement times are either to large or the additional hardware effort to expansive. In our work, we have developed a systematic approach how LED based solar simulators can be employed to perform full area measurements yielding spectral data with the same tool that is used for the power measurement. In particular, we propose an approach that can applied to any quasi-monochromatic light source with a finite spectral peak width independent of the peak shape. While we have demonstrated our approach on different photovoltaic technologies using a LED solar simulator for solar cells, an extension to full size photovoltaic modules is straight forward using a LED-based solar simulators for modules that have entered the market recently. This allows a detailed loss analysis of modules, e.g. the identification of degradation causes of photovoltaic modules in the field. As an extension to the EQE-measurement, we have furthermore demonstrated an approach that yields spatially resolved and wavelength dependent reflectivity data.

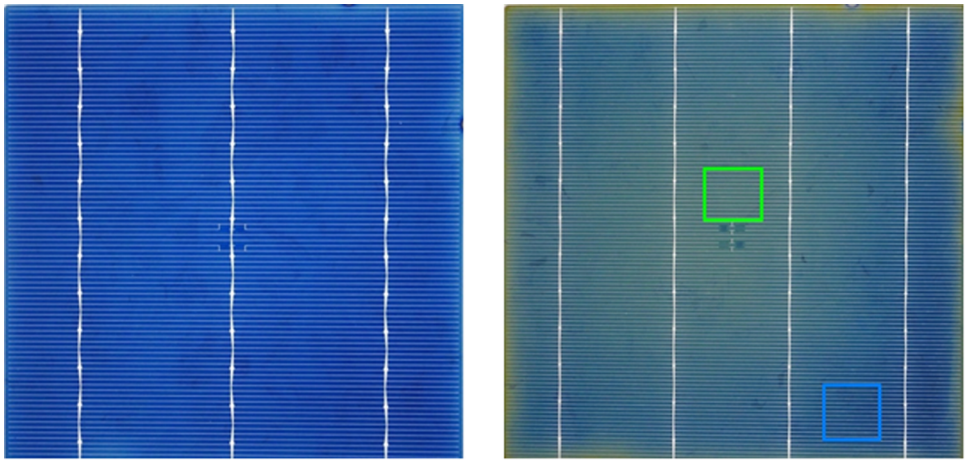

Fig. 7. Left: Solar cell used as reference for the reflectivity test. Right: Test cell with different test regions indicated.

In conclusion, we have provided two new measurement approaches that make use of the capabilities LED solar simulators and go beyond the standard current voltage characterization. Our rapid-EQE and rapid-reflectivity methods are based on a systematic mathematical analysis and quantitative correction schemes that include the spectral broadening of each individual LED channel. With demonstrated measurement times of less than one second, they are fully inline capable. Furthermore, they provide a full area assessment of solar cells and modules that does not require any additional hardware upgrades.

Acknowledgments

This work was supported by the German Federal Ministry of Economic Affairs and Energy (BMWi) within the research project CTM-100 (FKZ 0324033). The authors furthermore thank Stefan Eiternick for support with some of the measurements.

References

[1] S. Kohraku, K. Kurokawa, A fundamental experiment for discrete-wavelength LED solar simulator, Sol. Energy Mater. Sol. Cells 90 (2006) 3364.
[2] M. Bliss, T.R. Betts, R. Gottschalg, An LED-based photovoltaic measurement system with variable spectrum and flash speed, Sol. Energy Mater. Sol. Cells 93 (2009) 825.
[3] D. Kolberg, F. Schubert, N. Lontke, A. Zwigart, D.M. Spinner, Development of tunable close match LED solar simulator with extended spectral range to UV and IR, Energy Procedia 8 (2011) 100.
[4] M. Turek, S. Eiternick, J. Bauer, Ch. Hagendorf. Evaluation of the lateral uniformity of solar simulator light fields, in: Proceedings of the 35th EU PVSEC, 24 – 28 Sept., Brussels, Belgium. 2018.
[5] T. Luka, S. Eiternick, M. Turek, Rapid testing of external quantum efficiency using led solar simulators, Energy Procedia 77 (2015) 113.
[6] K. Sporleder C. Hagendorf M. Turek Rapid testing of spectrally resolved optical cell quality using led solar simulators, in: Proceedings of the 33rd EU PVSEC, 893, 2017.
[7] M. Turek, Current and illumination dependent series resistance of solar cells, J. Appl. Phys. 115 (2014).
[8] A. Paduthol, M. Juhl, T. Trupke, Correcting the effect of LED spectra on external quantum efficiency measurements of solar cells, IEEE J. Photovolt. 8 (2018) 559.
[9] G. Zaid, S.N. Park, S. Park, D.H. Lee, Differential spectral responsivity measurement of photovoltaic detectors with a light-emitting-diode-based integrating sphere source, Appl. Opt. 49 (2010) 6772.
[10] E.I. Stearns, R.E. Stearns, An example of a method for correcting radiance data for bandpass error, Color Res. Appl. 13 (1988) 257.
[11] J.L. Gardner, Bandwidth correction for LED chromaticity, Color Res. Appl. 31 (2006) 374.
[12] B. Fischer, Loss analysis of crystalline silicon solar cells using photoconductance and quantum efficiency measurements, Cuvillier Verl. Göttingen (2003).